from which they cannot. Therefore, it is this boundary that constitutes the limit to resolution in terms of the observations. Of course, hypothetical, errorless two-component observations to which a two-component model of the same family is fitted are on the side of the boundary corresponding to resolution. However, nonsystematic and systematic measurement errors may move this point to the other side of the boundary, where resolution is impossible since the solutions coincide. Systematic measurement errors influence the location of the point around which sets of observations are distributed. This point represents the expectations of the observations. The systematic errors may move this point close to the boundary. The kind of distribution of the nonsystematic errors defines how the sets of observations are distributed around this point. Therefore, the probability of resolution is determined by both types of errors combined.

BIBLIOGRAPHY

1. C. Chatfield, *Statistics for Technology,* 3rd ed., London: Chapman and Hall, 1995.
2. A. M. Mood, F. A. Graybill, and D. C. Boes, *Introduction to the Theory of Statistics,* 3rd ed., Auckland: McGraw-Hill, 1987.
3. A. Stuart and J. K. Ord, *Kendall's Advanced Theory of Statistics—Vol.1 Distribution Theory,* London: Arnold, 1994.
4. A. Stuart and J. K. Ord, *Kendall's Advanced Theory of Statistics—Vol. 2 Classical Inference and Relationship,* London: Arnold, 1991.
5. Anonymous, *Guide to the Expression of Uncertainty in Measurement,* 1st ed., Geneva: International Organization for Standardization, 1993.
6. W. H. Press et al., *Numerical Recipes in Fortran; the Art of Scientific Computing,* 2nd ed., New York: Cambridge University Press, 1992.
7. A. Grace, *Optimization Toolbox for Use With MATLAB™, USCL's Guide,* South Natick, MA: The Math Works, 1990.
8. R. I. Jennrich, *An Introduction to Computational Statistics,* Englewood Cliffs, NJ: Prentice-Hall, 1995.
9. A. van den Bos, Complex gradient and Hessian, *IEE Proceedings Vision and Image Signal Processing,* **141** (6): 380–382, 1994.
10. A. J. den Dekker and A. van den Bos, Resolution—A survey, *J. Opt. Soc. Am.,* **14** (3): 547–557, 1997.

ADRIAAN VAN DEN BOS
Delft University of Technology

MEASUREMENT OF FREQUENCY, PHASE NOISE AND AMPLITUDE NOISE

Frequency metrology has the highest resolution of all the measurement sciences. Simple systems readily achieve a fractional frequency resolution of 1 ppm (part per million) and some elaborate systems achieve 1 part in 10^{17} or less. Because of the readily achieved resolution, the growing trend is to convert the measurement of many different parameters to the measurement of frequency or frequency difference.

In the following we describe the basic ideas and definitions associated with various aspects of the specification and measurement of frequency, phase (or time), and the two components of spectral purity—phase modulation (PM) noise and amplitude modulation (AM) noise. The three topics are fundamentally linked, since as we will see below, frequency is proportional to the rate of change of phase with time, and the degree to which we can specify or measure signal phase, amplitude, or frequency is limited by the spectral purity of the signals.

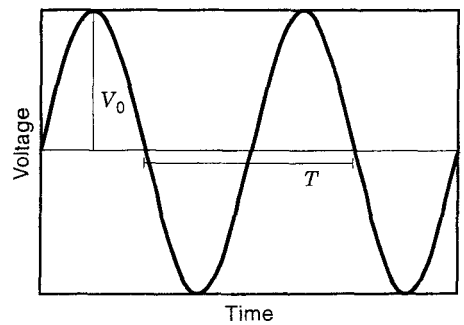

Figure 1. Output voltage of an ideal sinusoidal oscillator.

BASIC CONCEPTS AND DEFINITIONS

Figure 1 shows the output voltage signal of an ideal sinusoid oscillator as a function of time. The maximum value V_0 is the nominal amplitude of the signal. The time required for the signal to repeat itself is the period T of the signal. The nominal frequency ν_0 of the signal is the reciprocal of the period, $1/T$. This voltage signal can be represented mathematically by a sine function,

$$v(t) = V_0 \sin\theta = V_0 \sin(2\pi\nu_0 t) \tag{1}$$

where the argument $\theta = 2\pi\nu_0 t$ of the sine function is the nominal phase of the signal. The time derivative of the phase θ is $2\pi\nu_0$ and is called the nominal angular frequency ω_0. In the frequency domain, this ideal signal is represented by a δ function located at the frequency of oscillation.

In real situations, the output signal from an oscillator has noise. Such a noisy signal is illustrated in Fig. 2. In this example we have depicted a case in which the noise power is much less than the signal power. Fluctuations in the peak values of the voltage result in AM noise. Fluctuations in the zero crossings result in PM noise. Fractional frequency modulation (FM) noise refers to fluctuations in the period of the signal. Since the period (and thus the frequency) of the signal is related to the phase of the signal, FM noise and PM noise are directly related.

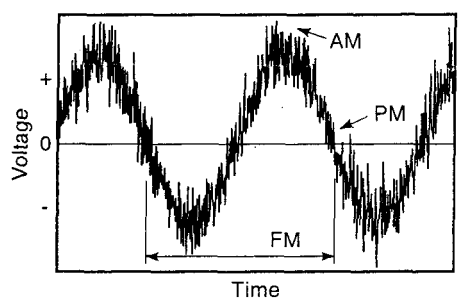

Figure 2. Output voltage of a noisy sinusoidal oscillator.

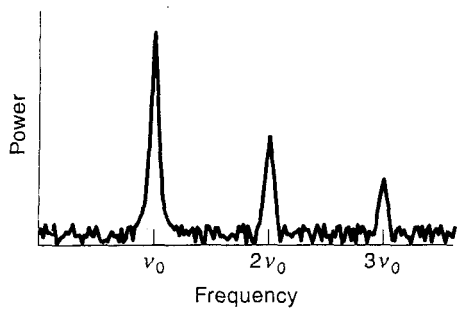

Figure 3. Power spectrum of a noisy signal.

Figure 3 shows the power spectrum of a noisy signal (power as a function of frequency) as measured by a spectrum analyzer. Although the maximum power occurs at the frequency of oscillation, other peaks are observed at frequencies of $2\nu_0$, $3\nu_0$, . . ., $n\nu_0$. These frequencies are called *harmonics* of the fundamental frequency ν_0; $2\nu_0$ is the second harmonic, $3\nu_0$ is the third harmonic, and so on. The power at these harmonic frequencies will depend on the design of the source. The spectrum around the fundamental frequency displays power sidebands at frequencies above the carrier (upper sideband) and at frequencies below the carrier (lower sideband). These power sidebands are the result of PM and AM noise in the signal. While the power spectrum gives an idea of the total noise of a signal, it does not give information about the relative magnitude of the PM and AM noise. Furthermore, at frequencies close to ν_0, it is difficult to separate noise power from the power of the fundamental frequency. Therefore, special measurement techniques are needed to measure PM and AM noise in oscillators.

Characterization of Frequency Stability and Amplitude Stability of a Signal

A noisy signal can be mathematically represented by

$$v(t) = [V_0 + \epsilon(t)]\sin[2\pi\nu_0 t + \phi(t)] \tag{2}$$

where $\epsilon(t)$ represents amplitude fluctuations (amplitude deviation from the nominal amplitude V_0) and $\phi(t)$ represents phase fluctuations (phase deviation from the nominal phase $2\pi\nu_0 t$) (1). The instantaneous frequency of this signal is defined as

$$\nu(t) = \frac{1}{2\pi}\frac{d}{dt}(\text{phase}) = \nu_0 + \frac{1}{2\pi}\frac{d}{dt}\phi(t) \tag{3}$$

Frequency fluctuations refer to the deviation of the instantaneous frequency from the nominal frequency: $\nu(t) - \nu_0$. Fractional frequency fluctuations, denoted as $y(t)$, refer to frequency fluctuations normalized to ν_0, that is,

$$y(t) = \frac{\nu(t) - \nu_0}{\nu_0} = \frac{1}{2\pi\nu_0}\frac{d}{dt}\phi(t) \tag{4}$$

Equation (4) indicates that there is a direct relation between phase fluctuations and fractional frequency fluctuations. Therefore if the PM noise of a signal is measured, the FM noise can be easily obtained and vice versa. The time deviation or fluctuation $x(t)$ of a signal is equal to the integral of $y(t)$ from 0 to t. This relation can be expressed as

$$y(t) = \frac{d}{dt}x(t) \tag{5}$$

Units of Measure for PM Noise, FM Noise, and AM Noise

Phase fluctuations in the frequency domain are characterized by the spectral density of the phase fluctuations $S_\phi(f)$, given by

$$S_\phi(f) = \text{PSD}[\phi(t)] = [\phi(f)]^2\frac{1}{\text{BW}} \tag{6}$$

where PSD refers to power spectral density, $[\phi(f)]^2$ is the mean-squared phase deviation at an offset frequency f from the frequency ν_0 (called the carrier in this context), and BW is the bandwidth of the measurement system (1–4). The offset frequency f is also called Fourier frequency. The units for $S_\phi(f)$ are rad²/Hz. Equation (6) is defined for $0 < f < \infty$; nevertheless it includes fluctuations from the upper and lower sidebands and thus is a double sideband unit of measure.

The PM noise unit of measure recommended by the IEEE (1,2,4) is $\mathscr{L}(f)$, defined as

$$\mathscr{L}(f) = \frac{S_\phi(f)}{2} \tag{7}$$

At Fourier frequencies far from the carrier frequency, where the integrated PM noise from ∞ to f (the Fourier frequency) is less than 0.1 rad², $\mathscr{L}(f)$ can be viewed as the ratio of phase noise power in a single sideband to power in the carrier (single-sideband phase noise). When $\mathscr{L}(f)$ is expressed in the form $10\log[\mathscr{L}(f)]$ its units are dB below the carrier in a 1 Hz bandwidth ($d\beta c$/Hz).

Frequency fluctuations in the frequency domain are characterized by the spectral density of the fractional frequency fluctuations $S_y(f)$, given by

$$S_y(f) = \text{PSD}[y(t)] = [y(f)]^2\frac{1}{\text{BW}} \tag{8}$$

where $y(f)^2$ represents the mean-squared fractional frequency deviation at an offset (Fourier) frequency f from the carrier. $S_y(f)$ is defined for Fourier frequencies $0 < f < \infty$, and its units are 1/Hz.

The conversion between $S_y(f)$ and $S_\phi(f)$ can be obtained from Eq. (4). Applying the Fourier transform to both sides of Eq. (4), squaring, and dividing by the measurement bandwidth result in

$$S_y(f) = \left(\frac{1}{2\pi\nu_0}\right)^2(2\pi f)^2 S_\phi(f) = \left(\frac{f}{\nu_0}\right)^2 S_\phi(f) \tag{9}$$

Amplitude fluctuations in the frequency domain are characterized by the spectral density of the fractional amplitude fluctuations $S_a(f)$, given by

$$S_a(f) = \text{PSD}\left(\frac{\epsilon(t)}{V_0}\right) = \left(\frac{\epsilon(f)}{V_0}\right)^2\frac{1}{\text{BW}} \tag{10}$$

where $\epsilon(f)^2$ represents the mean-squared amplitude deviation at an offset frequency f from the carrier (1). $S_a(f)$ is defined for Fourier frequencies $0 < f < \infty$, and its units are 1/Hz.

Figure 4(a) and 4(b) shows the common noise types characteristic of the PM noise and the AM noise of an oscillator (1,2,4–6).

Effects of Frequency Multiplication and Heterodyning on PM, FM, and AM Noise

When the frequency of a signal is multiplied by N, the phase fluctuations are also multiplied by N, as shown in Fig. 5(a).

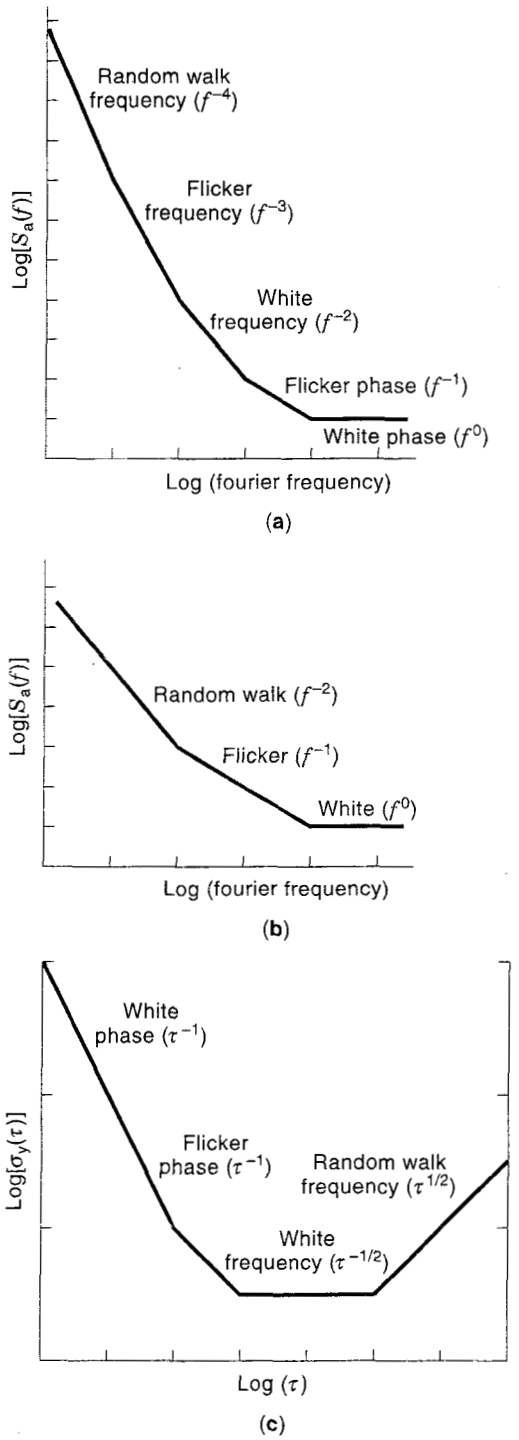

Figure 4. Common types of noise (fluctuations) in oscillators: (a) PM noise; (b) AM noise; (c) $\tau_y(\tau)$ (1,2,4–6).

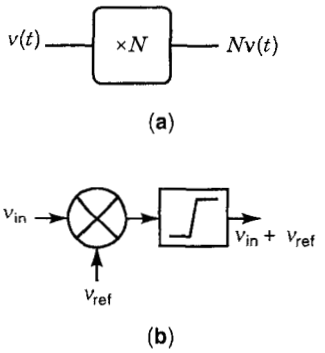

Figure 5. (a) Block diagram of a frequency multiplication system. (b) Block diagram of a frequency heterodyne or translation system.

The PM noise of the multiplied signal is given by

$$S_{\phi_2}(f) = \frac{[\phi_2(f)]^2}{\mathrm{BW}} + S_{\phi,M}(f) = \frac{N^2[\phi_1(f)]^2}{\mathrm{BW}} + S_{\phi,M}(f) = N^2 S_{\phi_1}(f) + S_{\phi,M}(f) \tag{11}$$

where $S_{\phi,M}(f)$ is the PM noise added by the frequency multiplier. Similarly, when the frequency of a signal is divided by N, the PM noise $S_\phi(f)$ of the divided signal is divided by N^2. Frequency multiplication and frequency division do not alter the fractional FM noise $S_y(f)$ of a signal since both the frequency fluctuations and the nominal frequency are multiplied by N, and the ratio remains constant (7). Ideally, frequency multiplication or division should not have an effect on AM noise either. Nevertheless, the AM noise of the multiplied or divided signal can be affected and determined by the multiplication or division scheme.

A system that translates or shifts the frequency of an input signal by a fixed frequency is shown in Fig. 5(b). In this system, a mixer is used to multiply the input and reference signals. The output signal after the high-pass filter has a frequency of $\nu_{in} + \nu_{ref}$. (Alternately the lower sideband $\nu_{in} - \nu_{ref}$ could just as well have been chosen.) The input frequency has been shifted by the frequency of the reference. The PM noise of the output signal of a frequency translation or frequency heterodyne system is given by

$$S_{\phi,o}(f) = S_{\phi,in}(f) + S_{\phi,ref}(f) + S_{\phi,T}(f) \tag{12}$$

where $S_{\phi,in}(f)$ is the PM noise of the input signal, $S_{\phi,ref}(f)$ is the PM noise of the reference, and $S_{\phi,T}(f)$ is the PM noise of the translator (in this case the mixer and the high-pass filter). The AM noise of the output signal will depend on the details of the translation scheme.

Time-Domain Fractional Frequency Stability of a Signal

In the time domain, the fractional frequency stability of a signal is usually characterized by the Allan variance, a type of

two-sample frequency variance given by

$$\sigma_y^2(\tau) = \frac{1}{2(N-2)\tau^2} \sum_{i=1}^{N-2} (x_{i+2} - 2x_{i+1} + x_i)^2 \tag{13}$$

$$\sigma_y^2(\tau) = \frac{1}{2(M-1)} \sum_{i=1}^{M-1} (\bar{y}_{i+1} - \bar{y}_i)^2 \tag{14}$$

$$\sigma_y^2(\tau) = \frac{2}{(\pi \nu_0 \tau)^2} \int_0^\infty S_\phi(f) \sin^4(\pi f \tau)\, df \tag{15}$$

where N is the number of time deviation samples, x_i is the time deviation over the interval τ, $M = N - 1$ is the number of frequency samples, and $\bar{y}_i$ is the fractional frequency deviation for interval i (1–4). Equation (13) is used when time data are available, Eq. (14) is used when frequency data are available, and Eq. (15) is used to convert frequency domain data (PM noise) to the time domain. The squared root of the Allan variance, $\sigma_y(\tau)$, is generally used to specify the frequency stability of a source. Figure 4(c) shows the slopes of the common noise types characteristic of the $\sigma_y(\tau)$ of oscillators. If the dominant noise type in short-term is flicker PM or white PM, the modified Allan variance given by Eq. (16), (17), or (18) can be used to improve the estimate of the underlying frequency stability of the sources (1,2,8):

$$\operatorname{mod} \sigma_y^2(\tau) = \frac{1}{2\tau^2 m^2 (N - 3m + 1)} \sum_{j=1}^{N-3m+1} \left(\sum_{i=j}^{m+j-1} (x_{i+2m} - 2x_{i+m} + x_i) \right)^2 \tag{16}$$

$$\operatorname{mod} \sigma_y^2(\tau) = \frac{1}{2(N - 3m + 1)} \sum_{j=1}^{N-3m+1} (\bar{y}'_{j+m} - \bar{y}'_j)^2 \tag{17}$$

$$\operatorname{mod} \sigma_y^2(\tau) = \frac{2}{m^4 (\pi \nu_0 \tau_0)^2} \int_0^\infty S_\phi(f) \frac{\sin^6(\pi \tau f)}{\sin^2(\pi \tau_0 f)}\, df \tag{18}$$

where

$$\bar{y}'_j = \frac{\bar{x}_{j+m} - \bar{x}_j}{\tau} \tag{19}$$

and

$$\bar{x}_j = \frac{\sum_{k=0}^{m-1} x_{j+k}}{m} \tag{20}$$

Here $\bar{x}_j$ is the phase (time) averaged over n adjacent measurements of duration τ_0. Thus mod $\sigma_y(\tau)$ is proportional to the second difference of the phase averaged over a time $m\tau_0$. Viewed from the frequency domain, mod $\sigma_y(\tau)$ is proportional to the first difference of the frequency averaged over m adjacent samples.

The confidence intervals for $\sigma_y(\tau)$ and mod $\sigma_y(\tau)$ as a function of noise type and the number of samples averaged are discussed in Refs. 1 and 4.

MEASUREMENT SYSTEMS

Direct Measurements

Direct Measurements of Frequency and Frequency Stability Using a Counter. Figure 6 shows the timing diagram for the direct measurement of signal frequency relative to a reference frequency using a counter. The normal convention is to start with the signal under test and stop with the reference. The user typically chooses the nominal measurement period, which is an integral number of cycles of the reference. For example $\tau = N_{\text{ref}}/\nu_{\text{ref}} \cong 1$ s. The instrument counts N_{sig}, the nominal number of cycles of the signal under test that occur before the reference signal stops the count. The frequency of the signal averaged over a measurement interval τ is given by

$$\nu_{\text{sig}}(\tau) = N_{\text{sig}}(\tau) \frac{\nu_{\text{ref}}}{N_{\text{ref}}} \tag{21}$$

where ν_{ref} is the frequency of the reference. Since the measured signal frequency is proportional to the time base or reference frequency, an error in the time-base frequency leads to a proportional error in the determination of the signal frequency.

The intrinsic fractional frequency resolution of a simple counter is $\pm 1/N_{\text{sig}}$. Some sophisticated counters have interpolation algorithms that allow them to improve the intrinsic resolution by a factor of β, which can be 100 or more. If the frequency of the signal under test is less than the frequency of the reference, the resolution can often be improved by reversing the roles of the signal and reference. The counter reading can then be inverted to find the frequency of the signal.

The uncertainty in the frequency from a particular measurement taken over a measurement time τ is the intrinsic resolution plus the combined fractional instability of signal $\sigma^2_{y,\text{sig}}(\tau)$ and the reference $\sigma^2_{y,\text{ref}}(\tau)$. When these factors are inde-

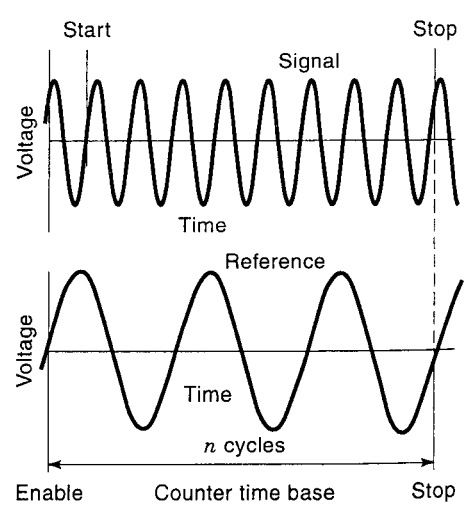

Figure 6. Timing diagram for a direct frequency measurement system.

pendent, they are added in quadrature:

frequency uncertainty

$$= \frac{\Delta\nu(\tau)}{\nu} = \left[\left(\frac{1}{\beta N_{\text{sig}}}\right)^2 + \sigma^2_{y,\text{ref}}(\tau) + \tau^2_{y,\text{sig}}(\tau)\right]^{1/2} \tag{22}$$

The time-domain fractional frequency stability of the signal $\sigma^2_{y,\text{sig}}(\tau)$ relative to the frequency stability of the reference can be estimated from a series of consecutive frequency measurements using Eq. (14) (1,2). There is often dead time between frequency measurements in the direct method, which leads to biases in the estimation of fractional frequency stability; these biases depend on noise type (9). More elaborate techniques that eliminate this bias and offer better intrinsic frequency resolution are described in later sections on heterodyne measurements.

Direct Measurements of Phase or Time Using a Counter. For sinusoidal signals, phase or time is usually referenced to the positive-going zero crossing of the signal. For digital signals, time is usually referenced to the mean of the 0 and the 1 states at the positive-going transition. Although the counter can be started with the signal or the reference, we usually start with the signal. Then advancing phase (time) corresponds to a signal frequency that is higher than the reference. The instrument counts N_{ref}, the nominal number of cycles of the counter time base frequency ν_{ref} that occur before the reference signal stops the count. The phase of the signal relative to the reference is

$$\theta_{\text{sig}} = 2\pi N_{\text{ref}} \frac{\nu_{\text{sig}}}{\nu_{\text{ref}}} \tag{23}$$

where ν_{sig} is the frequency of the signal. The time of the signal relative to the reference is

$$t_{\text{sig}} = \frac{N_{\text{ref}}}{\nu_{\text{ref}}} \tag{24}$$

Since the measured phase (time) is proportional $1/(\nu_{\text{ref}})$, an error in the time base (reference) frequency leads to an error in the determination of the signal phase. There may also be phase errors or time errors in the measurement due to the voltage standing wave ratio (VSWR) on the transmission lines to the counter from the signal and the reference (10).

For a simple counter the intrinsic phase resolution is $2\pi\nu_{\text{sig}}/\nu_{\text{ref}}$, while the time resolution is $1/\nu_{\text{ref}}$. Some sophisticated counters have interpolation algorithms that allow them to improve the intrinsic resolution by a factor of β, which can be 100 or more.

The uncertainty in the measurement of phase $\Delta\phi$ or time ΔT using this approach is given by the intrinsic resolution plus the combined fractional instability of signal $\sigma^2_{y\text{sig}}(\tau)$ and the reference $\sigma^2_{y\text{ref}}(\tau)$. When these factors are independent, they are added in quadrature:

$$\Delta\phi = \theta_{\text{sig}}\left[\left(\frac{1}{N_{\text{ref}}\beta}\right)^2 + \sigma^2_{y\text{ref}}(\tau) + \sigma^2_{y\text{sig}}(\tau)\right]^{1/2} \tag{25}$$

$$\Delta T = t_{\text{sig}}\left[\left(\frac{1}{N_{\text{ref}}\beta}\right)^2 + \sigma^2_{y\text{ref}}(\tau) + \sigma^2_{y\text{sig}}(\tau)\right]^{1/2} \tag{26}$$

The time-domain fractional frequency stability of the signal $\sigma^2_{y\text{sig}}(\tau)$ relative to the frequency stability of the reference can be estimated from a series of consecutive phase measurements separated by a time τ, using Eq. (13) (1,2). More elaborate techniques that offer better resolution are described in later sections on heterodyne measurements.

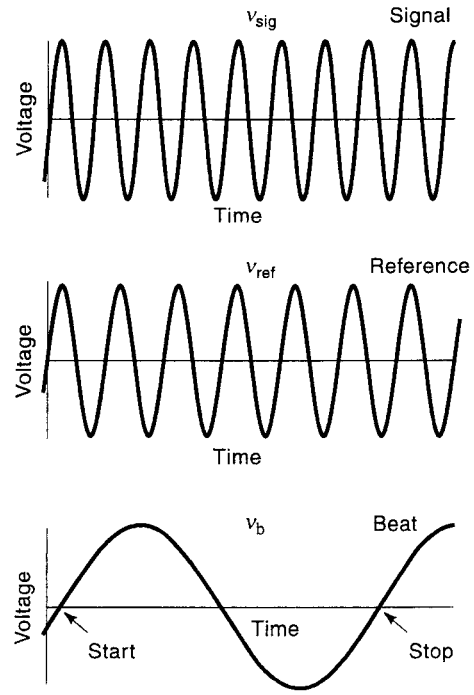

Figure 7. Timing diagram of a heterodyne time measurement system.

Heterodyne Measurements

Heterodyne techniques offer greatly improved short-term resolution over direct measurement techniques of frequency, phase, and time (see Fig. 7). In this technique the signal under test is heterodyned against the reference signal ν_{ref} and the difference frequency or beat frequency (lower curve) ν_b measured. The frequency resolution is improved by a factor ν_{ref}/ν_b over direct measurements.

Heterodyne Measurements of Frequency. Using the heterodyne method, the frequency of the signal source is

$$\nu_{\text{sig}} = \nu_{\text{ref}} \pm \nu_b \tag{27}$$

Additional measurements are required to determine the sign of the frequency difference. The usual method is to change the frequency of the reference by a known amount and determine whether the beat becomes smaller or larger. The resolution for frequency measurements is given by

$$\frac{\Delta\nu}{\nu_{\text{ref}}} = \Delta t \frac{\nu_b^2}{\nu_{\text{ref}}} \tag{28}$$

where Δt is the timing resolution. The uncertainty is limited by the frequency stability of the reference and the phase variations of the phase detector. The minimum time between data

samples is $1/\nu_b$ for clocks that are nearly at the same frequency (a limitation in many situations).

Fifty percent of the time this approach is insensitive to the phase fluctuation between the signal and the reference. This down time, called "dead time" (5,9), biases the calculation of $\sigma_y(\tau)$ and mod $\sigma_y(\tau)$ by an amount that depends on the noise type and the duration of the dead time. Bias tables as a function of noise type and percent dead time are given in Ref. 9. The dead-time limitation can be circumvented by using two counters triggered on alternate cycles of ν_b.

Heterodyne Measurements of Phase (Time). The resolution for heterodyne measurements of time or phase is increased to

$$\Delta\tau = \frac{\nu_b}{\nu_{ref}}\Delta t \tag{29}$$

where Δt is the timing resolution of the counter. To avoid ambiguity ν_b should be larger than the frequency fluctuations of both the reference and the source under test. Additional measurements are required to determine if the frequency of the source is higher or lower than the reference. The phase of the beat signal goes through zero when the phase difference between the two signals is $\pm(2n + 1) \times 90°$ where $n = 0, 1, 2, 3, \ldots$. The time of the zero crossing is biased or in error by $\Delta\phi$ due to imperfections in the symmetry of the phase detector and/or the VSWR in the reference and signal paths (10). Timing errors due to VSWR effects and typical temperature coefficients for mixer biases are given in Ref. 10 for frequencies of 5 and 100 MHz. These errors generally scale as $1/\nu_{sig}$.

The time of the source under test is

$$t_{sig} = T_{ref} \pm \frac{n}{\nu_{ref}} \pm \Delta\phi \tag{30}$$

where n is the number of beat cycles that have occurred since the original synchronization. The minimum time between data samples is $1/\nu_b$. For clocks that are at nearly the same frequency, this limitation can be very restrictive.

The time-difference data can be used to characterize the fractional frequency stability of the sources using Eq. (13). The resolution for short-term time domain frequency stability (τ less than 0.1 s) is typically much worse than that obtained from integrating the phase noise using Eq. (15) (8,11)

Basic Configuration of PM and AM Noise Measurement Systems

Figure 8 shows the basic building block used in PM and AM noise measurement systems. It consists of a phase shifter, a mixer, and a low-pass filter. The two input signals to the mixer can be represented as

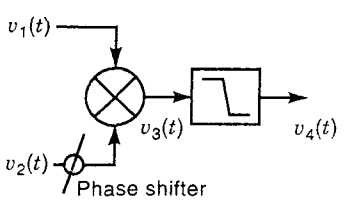

Figure 8. Basic building block for AM and PM noise measurement systems.

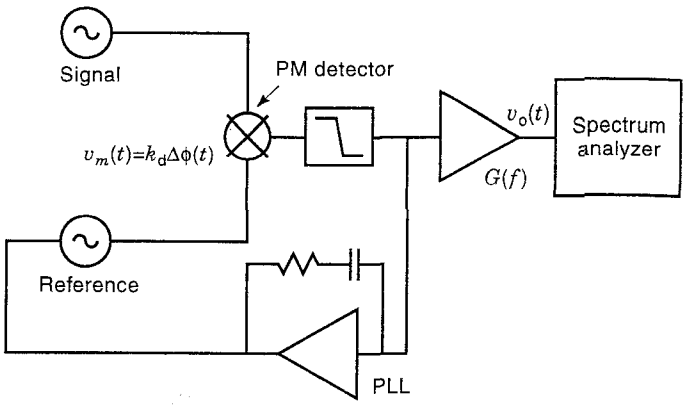

Figure 9. Block diagram for a heterodyne (two-oscillator) PM noise measurement system.

$$\begin{aligned} v_1(t) &= A_1(t)\cos[2\pi\nu_0 t + \Phi_1(t)] \\ &= [V_1 + \epsilon_1(t)]\cos[2\pi\nu_0 t + \phi_1 + \phi_1(t)] \end{aligned} \tag{31}$$

$$\begin{aligned} v_2(t) &= A_2(t)\cos[2\pi\nu_0 t + \Phi_2(t)] \\ &= [V_2 + \epsilon_2(t)]\cos[2\pi\nu_0 t + \phi_1 + \phi_2(t)] \end{aligned} \tag{32}$$

where $\epsilon_1(t)$ and $\epsilon_2(t)$ represent the amplitude fluctuations of the signals and $\phi_1(t)$ and $\phi_2(t)$ represent the phase fluctuations of the signals. For an ideal mixer, the signal $v_3(t)$ is equal to the product of signals $v_1(t)$ and $v_2(t)$. After some algebraic manipulation, we have

$$\begin{aligned} v_3(t) = \frac{A_1(t)A_2(t)}{2}\{&\cos[4\pi\nu_0 t + \Phi_1(t) + \Phi_2(t)] \\ &+ \cos[\Phi_1(t) - \Phi_2(t)]\} \end{aligned} \tag{33}$$

At the output of the low-pass filter, the signal reduces to

$$v_4(t) = \frac{A_1(t)A_2(t)}{2}\{\cos[\Delta\phi + \Delta\phi(t)]\} \tag{34}$$

where $\Delta\phi$ is the difference between the phase angles of the two input signals ($\phi_1 - \phi_2$) and $\Delta\phi(t) = \phi_1(t) - \phi_2(t)$. When $\Delta\phi$ is approximately equal to an odd multiple of $\pi/2$ and the integrated phase noise $[\int \Delta\phi(f)^2\, df]$ does not exceed 0.1 rad^2, the two signals are in quadrature and the output voltage of the mixer is proportional to the difference of the phase fluctuations in the signals $v_1(t)$ and $v_2(t)$. When a double-balanced mixer is used, the amplitude fluctuations are suppressed by 25 to 40 dB (11,12). This is also called suppression of AM to PM conversion in a double-balanced mixer.

When the two input signals to the mixer are in phase or $\Delta\phi \cong 0$, the output voltage of the mixer is proportional to the amplitude fluctuations of the signals. The suppression of phase fluctuations when $\Delta\phi \cong 0$ is higher than 90 dB (11,12). The setup in Fig. 8 can be used in either AM noise or PM noise measurement systems by adjusting the phase shifter.

PM Noise Measurement Systems For Oscillators and Amplifiers

Heterodyne Measurements of PM Noise in Signal Sources (Two-Oscillator Method). Figure 9 shows a heterodyne PM noise measurement system for an oscillator. In this system, the signals from the test oscillator and a reference oscillator of simi-

lar frequency are fed into a double-balanced mixer. A phase-locked loop (PLL) is used to lock the reference frequency to the test oscillator frequency and to maintain quadrature between the two input signals to the mixer (13). The output voltage of the mixer is proportional to the difference between the phase fluctuations of the two sources. This voltage is amplified and its PSD is measured with a spectrum analyzer. Often this spectrum analyzer is of the fast Fourier transform (FFT) type. The voltage at the output of the amplifier is

$$v_o(t) = k_d G \Delta\phi(t) \tag{35}$$

where k_d is the mixer's phase-to-voltage conversion factor (or mixer sensitivity), G is the gain of the amplifying stage, and $\Delta\phi(t)$ is the difference between the phase fluctuations of the test oscillator and the reference $[\phi_A(t) - \phi_B(t)]$. The PM noise can be obtained from

$$S_\phi(f) = \frac{\mathrm{PSD}[v_o(t)]}{(k_d G)^2} \tag{36}$$

The calibration factor or mixer sensitivity k_d can be found by turning off the PLL to obtain a beat frequency signal at the mixer output. The slope at the zero crossing and the period of this signal can be measured with an oscilloscope or another recording device. The calibration factor k_d in V/rad is

$$k_d = (\text{slope}) \times \frac{T}{2\pi} \tag{37}$$

Ideally this measurement should be made at the output of the amplifier because the measurement then yields $k_d G$, which includes the effect of amplifier input impedance on the performance of the mixer. The calibration of this PM noise measurement system using the beat-frequency method can introduce errors in the measurement if the mixer and the amplifier gains are frequency dependent, as is often the case. Figure 10 shows the variation of k_d with Fourier frequency for different mixer terminations. Capacitive terminations improve the mixer sensitivity, thereby improving the noise floor. However, the frequency response is not nearly as constant as the response obtained with resistive terminations, thus increasing the measurement error (11).

A calibrated Gaussian noise source centered about the carrier frequency can be used to calibrate the frequency-dependent errors (14,15). In this technique Gaussian noise is added to the reference signal by means of a low-noise power summer. Since the Gaussian noise is independent of the reference noise, equal amounts of PM and AM noise are added to the reference signal. When the Gaussian noise is "on," the PSD of the output noise voltage $v_o(t)$ is equal to

$$\mathrm{PSD}[v_{o,\mathrm{on}}(t)] = (k_d G)^2 S_{\mathrm{PMcal}} \tag{38}$$

where S_{PMcal} is the PM noise added by the Gaussian noise source. The calibration factor as a function of frequency is obtained dividing $\mathrm{PSD}[v_{o,\mathrm{on}}(t)]$ by S_{PMcal}. A PSD measurement is then made with the Gaussian noise "off." The calibrated PM noise is obtained from

$$S_\phi(f) = \frac{\mathrm{PSD}[v_{o,\mathrm{off}}(t)]}{(k_d G)^2} = S_{\mathrm{PMcal}} \frac{\mathrm{PSD}[v_{o,\mathrm{off}}(t)]}{\mathrm{PSD}[v_{o,\mathrm{on}}(t)]} \tag{39}$$

This approach greatly reduces the uncertainty of the measurement because it automatically takes into account the frequency-dependent errors. This approach also reduces the time necessary to make routine PM noise measurements as compared to traditional methods since the measurement is now reduced to a simple ratio measurement between noise on and noise off (14,15). The use of this calibration technique is illustrated in the cross-correlation measurements discussed in the following and shown in Fig. 11.

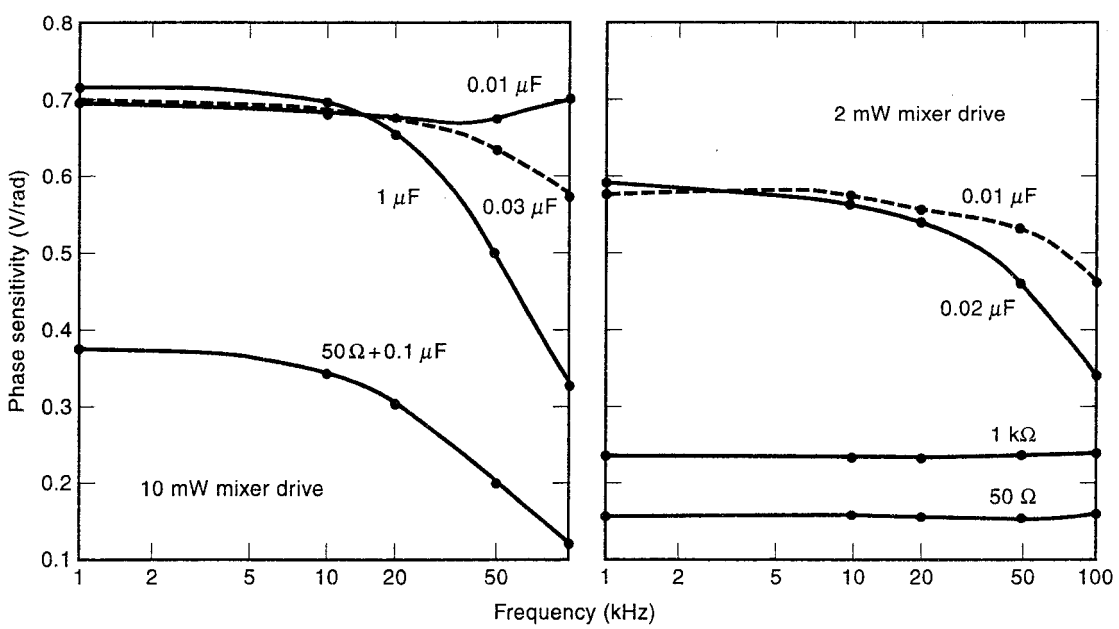

Figure 10. Sensitivity of a low-level double-balanced mixer at 5 MHz as a function of the intermediate frequency (IF) port termination for radio frequency (RF) and local oscillator (LO) inputs of +2 and +10 dBm (11).

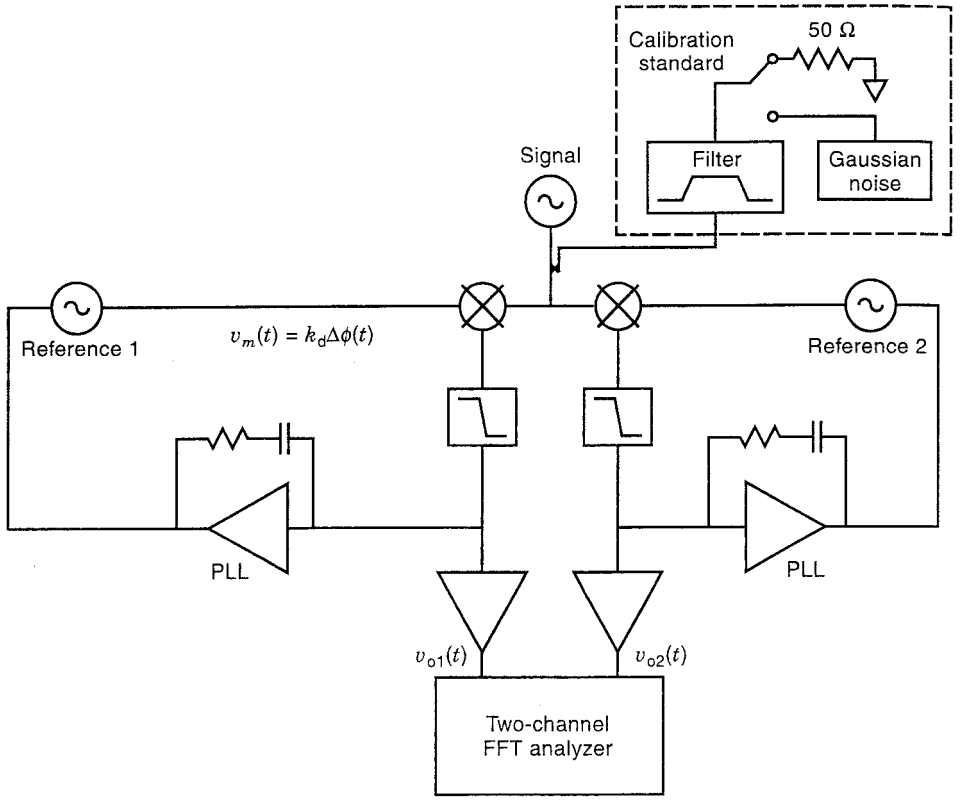

Figure 11. Block diagram of a two-channel cross-correlation system for measuring PM noise in an oscillator. Calibration of the system is accomplished using a PM and AM noise standard (14,15).

The confidence intervals for spectrum analyzers (swept and FFT) as a function of the number of measurements can be estimated from Table 1 (4,16–18). Biases in commonly used FFT window functions are discussed in Ref. 4.

One of the shortcomings of the single-channel, two-oscillator measurement system is that the measured noise includes noise contribution from the test source as well as that from the reference source. The noise terms included in $S_\phi(f)$ are

$$S_\phi(f) = S_{\phi,\mathrm{A}}(f) + S_{\phi,\mathrm{B}}(f) + \frac{v_\mathrm{n}^2(f)}{k_\mathrm{d}^2\mathrm{BW}} + S_{\mathrm{a,A}}(f)\beta_\mathrm{A}^2 + S_{\mathrm{a,B}}(f)\beta_\mathrm{B}^2 \tag{40}$$

Table 1. Approximate Statistical Confidence Interval for FFT and Swept Spectrum Analyzers (16–18). β = N (the Number of Averages) for FFT Analyzers and β = N(RBW/VBW) for Swept Spectrum Analyzers. (RBW Refers to the Resolution Bandwidth of the Spectrum Analyzer and VBW refers to the video bandwidth).

β	69% Confidence Interval (dB)		95% Confidence Interval (dB)	
4	−2	+3	−3	+6
6	−1.5	+2.3	−2.5	+5
10	−1.2	+1.7	−2	+4
30	−0.72	+0.88	−1.3	+1.8
100	−0.41	+0.46	−0.76	+0.92
200	−0.3	+0.32	−0.54	−0.63
1,000	−0.13	+0.13	−0.25	−0.27
3,000	−0.08	+0.08	−0.15	+0.15
10,000	−0.04	+0.04	−0.08	+0.08

where $S_{\phi,\mathrm{A}}(f)$ is the PM noise of the test source, $S_{\phi,\mathrm{B}}(f)$ is the PM noise of the reference, $v_\mathrm{n}(f)$ is the noise added by the mixer, the amplifier, and the spectrum analyzer, $S_{\mathrm{a,A}}(f)$ and $S_{\mathrm{a,B}}(f)$ refer to the AM noise of the test source and the reference, and β_A and β_B are the factors by which the AM noise is suppressed. If the PM noise of the reference is higher than the PM noise of the test source, then the PM noise of the source cannot be measured accurately.

The last three terms of Eq. (40) constitute the noise floor of the measurement system. The noise floor can be estimated by using a single source (test source or reference) to feed the two inputs of the mixer. A phase shifter placed in one of the channels is used to adjust the phase difference to an odd multiple of 90°. The PM noise of the driving source is mostly canceled and the measured noise at the output is

$$S_\phi(f) = \frac{v_\mathrm{n}^2(f)}{k_\mathrm{d}^2\mathrm{BW}} + 2S_{\mathrm{a,A}}(f)\beta_\mathrm{A}^2 + \eta(f)S_{\phi,\mathrm{A}}(f) \tag{41}$$

where the factor $\eta(f)$ is due to decorrelation of the source noise and is much smaller than 1 for small Fourier frequencies. [See the section on delay line measurements, especially Eq. (52), for a discussion of this effect.] Equation (41) is approximately equal to the noise-floor components in Eq. (40). Equation (40) indicates that the AM noise of the source and the reference can affect PM noise measurements; thus sources with low AM noise should be used.

Cross-Correlation Heterodyne Measurements of PM Noise in Signal Sources. One of the limitations of the single-channel, two-oscillator method is that the PM noise of the reference contributes to the measured noise. If three different oscilla-

tors are available (A, test source; B, reference 1; C, reference 2), PM noise measurements of three different pairs of oscillators can be made and the PM noise of the source can be approximated by

$$S_{\phi,\mathrm{A}}(f) \cong \tfrac{1}{2}[S_{\phi,\mathrm{AB}}(f) + S_{\phi,\mathrm{AC}}(f) - S_{\phi,\mathrm{BC}}(f)] - 2S_{\mathrm{a,A}}(f)\beta_{\mathrm{A}}^2 - \frac{v_{\mathrm{n}}^2(f)}{k_{\mathrm{d}}^2\mathrm{BW}} \tag{42}$$

where $S_{\phi,\mathrm{AB}}(f)$ includes the PM noise of sources A and B, $S_{\phi,\mathrm{AC}}(f)$ includes the PM noise of sources A and C, and $S_{\phi,\mathrm{BC}}(f)$ includes the PM noise of sources B and C. One problem with this approach is that small errors in any of the three measurements taken separately can result in large overall errors. Another problem is that the noise of the measurement system still contributes to the noise floor.

A more effective way of eliminating the PM noise from the reference is to use cross-correlation PM noise measurements. Figure 11 shows a two-channel, cross-correlation PM noise measurement system that uses two reference oscillators and two PM noise detectors operating simultaneously. Each individual channel is a simple heterodyne measurement system. Therefore the noise terms in $\mathrm{PSD}[v_{\mathrm{o1}}(t)]$ and $\mathrm{PSD}[v_{\mathrm{o2}}(t)]$ divided by the respective calibration factors are described by Eq. (40). The PSD of the cross-correlation of the noise voltages $v_{\mathrm{o1}}(t)$ and $v_{\mathrm{o2}}(t)$ divided by the calibration factor is

$$S_\phi(f) = S_{\phi,\mathrm{A}}(f) + S_{\mathrm{a,A}}(f)\beta_{\mathrm{A}}^2 + \frac{1}{\sqrt{N}}\left(S_{\phi,\mathrm{B}}(f) + S_{\phi,\mathrm{C}}(f) + \frac{v_{\mathrm{n}}^2(f)}{k_{\mathrm{d}}^2\mathrm{BW}}\right) + S_{\mathrm{a,B}}(f)\beta_{\mathrm{B}}^2 + S_{\mathrm{a,C}}(f)\beta_{\mathrm{C}}^2 \tag{43}$$

where $S_{\phi,\mathrm{A}}(f)$ is the PM noise of the test source, $S_{\phi,\mathrm{B}}(f)$ and $S_{\phi,\mathrm{C}}(f)$ are the PM noise of the references, and N is the number of averages in the measurement (11,14,15,19,20). The contribution of the PM noise of the references and the noise in the detectors and amplifiers are reduced by $\sqrt{N}$, because they are independent. This results in a reduction of the unwanted PM noise in the references and the measurement system of 10 dB for 100 averages and 20 dB for 10,000 averages. This powerful measurement technique makes it possible to obtain an accurate measurement of the PM noise of a source that has lower noise than the references if the AM noise of the source can be neglected.

Heterodyne Measurements of PM Noise in Amplifiers. Figure 12 shows the block diagram of a PM noise measurement system for a pair of amplifiers. In this system an oscillator signal is split using a reactive power splitter. The outputs of the splitter drive two test amplifiers, and their outputs feed a double-balanced mixer. The mixer output is then amplified and measured by a spectrum analyzer. A phase shifter in one of the channels is used to maintain quadrature. The PM noise of the amplifier pair is obtained dividing the PSD of the noise voltage $v_{\mathrm{o}}(t)$ by the calibration factor $(k_{\mathrm{d}}G)^2$,

$$S_\phi(f) = \frac{\mathrm{PSD}[v_{\mathrm{o}}(t)]}{(k_{\mathrm{d}}G)^2} = S_{\phi,\mathrm{amp}}(f) + \frac{v_{\mathrm{n}}^2(f)}{k_{\mathrm{d}}^2\mathrm{BW}} + S_{\mathrm{a}}(f)\beta^2 \tag{44}$$

where $S_{\phi,\mathrm{amp}}(f)$ is the PM noise of the amplifier pair and $S_{\mathrm{a}}(f)$ is the AM noise of the source. This system assumes that the noise of the amplifiers is higher than the noise floor of the measurement system. If this is not the case, cross-correlation measurement systems should be used. The calibration factor can be easily obtained by adding a Gaussian noise source to one of the channels and making measurements with the noise on and the noise off, as discussed previously. Calibration can also be achieved by using a second source to drive one of the amplifiers to obtain a beat signal at the output of the mixer. An oscilloscope can then be used to measure the zero-crossing slope and the period of the beat signal, and the calibration factor can be computed using Eq. (37).

A similar measurement system can be used to measure the PM noise of a single amplifier if the delay across the amplifier is so small that decorrelation of the source noise is not important to the measurement. See Eq. (52) and associated text for a discussion of decorrelation effects.

Cross-Correlation Heterodyne Measurements of PM Noise in Amplifiers. Figure 13 shows a cross-correlation PM noise measurement system for a pair of amplifiers. It consists of two channels, each a separate heterodyne measurement system. The PSD of the cross-correlation of the noise voltages $v_{\mathrm{o1}}(t)$ and $v_{\mathrm{o2}}(t)$ divided by the calibration factor is

$$S_\phi(f) = \frac{\mathrm{PSD}[v_{\mathrm{o1}}(t)v_{\mathrm{o2}}(t)]}{(k_{\mathrm{d}}G)^2} = S_{\phi,\mathrm{amp}}(f) + \frac{1}{\sqrt{N}}\frac{v_{\mathrm{n}}^2(f)}{(k_{\mathrm{d}}G)^2\mathrm{BW}} + S_{\mathrm{a,A}}(f)\beta_{\mathrm{A}}^2 \tag{45}$$

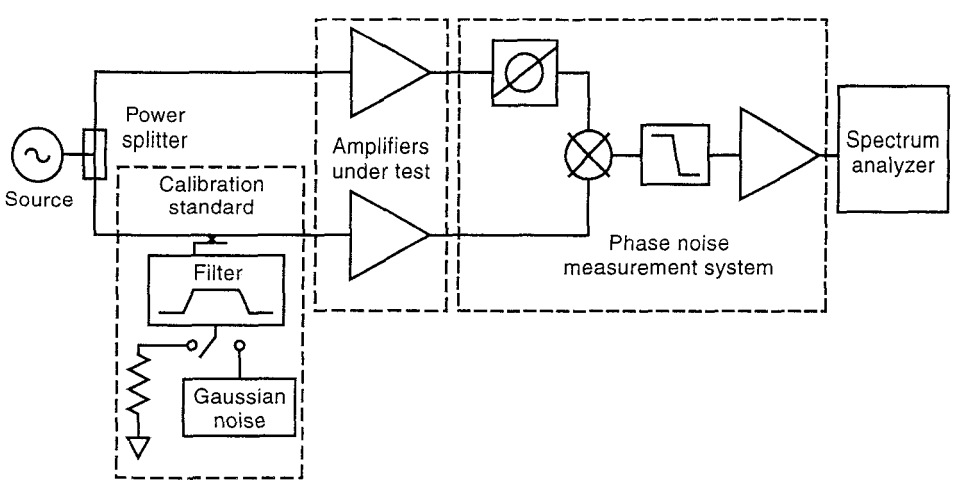

Figure 12. Block diagram of a single-channel system for measuring PM noise in a pair of amplifiers.

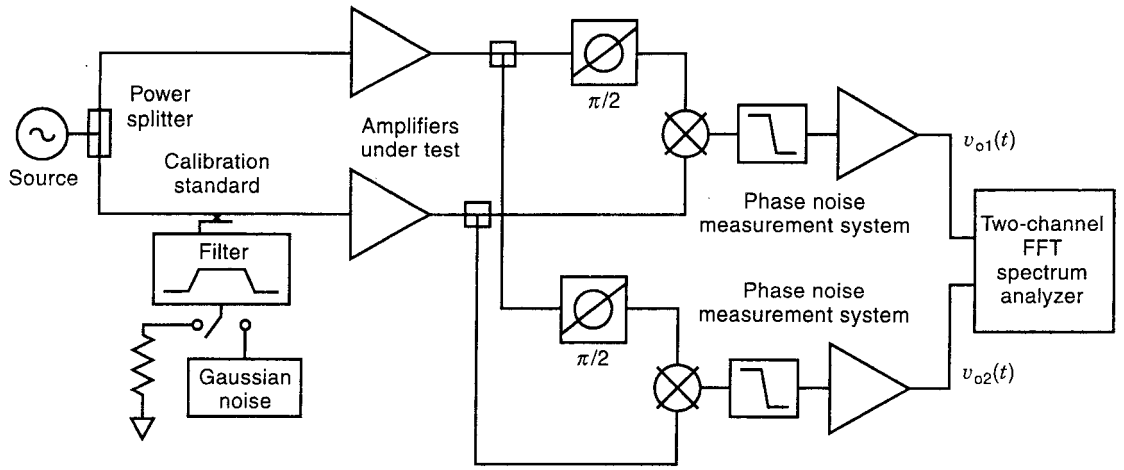

Figure 13. Block diagram of a two-channel cross-correlation system for measuring PM noise in a pair of amplifiers.

The noise added by the phase detectors is reduced by $\sqrt{N}$. The calibration factor k_dG can be obtained by adding a calibrated Gaussian noise source about the carrier frequency as shown in Fig. 13. In this setup the noise floor is generally limited by the AM noise of the source. It is therefore important to select a source with low AM noise and to operate the mixer at the maximum point of AM rejection.

Delay-Line Measurements of PM Noise in Signal Sources. A PM noise measurement system that does not need a second source is the delay-line system shown in Fig. 14 (11,21). In this setup the oscillator signal is split, a delay line of time delay τ_d is placed in one channel, and a phase shifter is placed in the other channel. The two channels are fed into a double-balanced mixer. The phase fluctuations of the combined signal at the mixer output are given by

$$\phi_m(f) = [2 - 2\cos(2\pi f\tau_d)]^{1/2}\phi(f) \tag{46}$$

where $\phi(f)$ are the rms phase fluctuations of the source at an offset frequency f (21,22). If the phase shifter is adjusted so that the phase difference between the two input signals is an odd multiple of 90°, then the output voltage of the mixer is proportional to the phase fluctuations of the source. For $2\pi f\tau_d \ll 1$,

$$v_m(f) \cong k_d\left[2 - 2\left(1 - \frac{(2\pi f\tau_d)^2}{2}\right)\right]^{1/2}\phi(f) = k_d 2\pi f\tau_d\phi(f) \tag{47}$$

where $v_m(f)$ is the output voltage of the mixer at an offset frequency f. Equation (47) can also be expressed in terms of $y(f)$ by multiplying the right side by ν_0/f:

$$v_m(f) \cong k_d 2\pi\nu_0\tau_d y(f) \tag{48}$$

Equation (48) can be equivalently expressed in the time domain as

$$v_m(t) \cong k_d 2\pi\nu_0\tau_d y(t) \tag{49}$$

Equation (49) indicates that the output voltage of the mixer is proportional to the frequency fluctuations in the source, and thus this system measures the FM noise of the test source. The voltage at the output of the amplifier is given by

$$v_o(t) \cong k_d(2\pi\nu_0\tau_d)Gy(t) = \nu_0 k_\nu Gy(t) \tag{50}$$

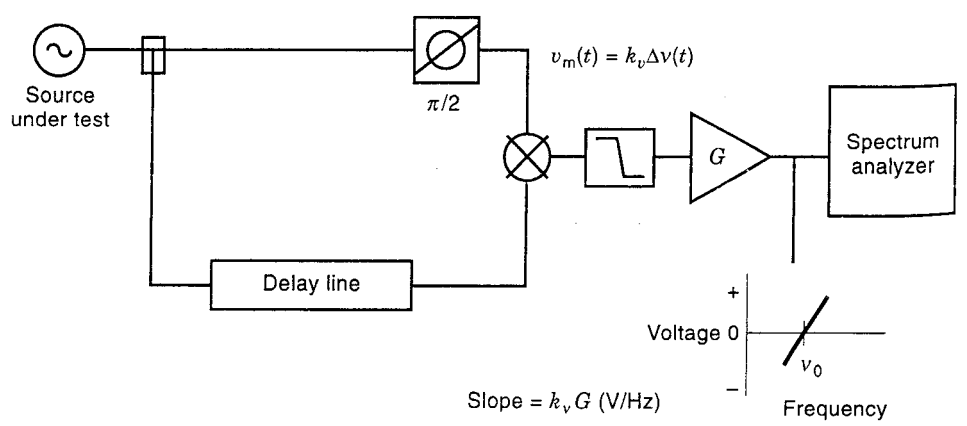

Figure 14. Block diagram of a PM noise measurement system that uses a delay line to measure PM noise in an oscillator.

where k_ν is the mixer sensitivity to frequency fluctuations and G is the voltage gain of the amplifier. The FM and PM noise of the source can then be obtained:

$$S_y(f) \cong \frac{\mathrm{PSD}[v_o(t)]}{(2\pi \nu_0 \tau_d k_d G)^2} = \frac{\mathrm{PSD}[v_o(t)]}{(\nu_0 k_\nu G)^2} \tag{51}$$

$$S_\phi(f) \cong \frac{\mathrm{PSD}[v_o(t)]}{(2\pi f \tau_d k_d G)^2} = \left(\frac{1}{f}\right)^2 \frac{\mathrm{PSD}[v_o(t)]}{(k_\nu G)^2} \tag{52}$$

Equations (51) and (52) are valid only for $f \ll 1/(2\pi\tau_d)$, where the approximation in Eq. (47) is valid. The calibration factor k_ν can be found by stepping the source frequency up and down and measuring the corresponding voltage change at the output of the amplifier. The voltage change divided by the frequency change is equal to $k_\nu G$ in V/Hz. At $f > 1/(2\tau_d)$, the output of the mixer is approximately sinusoidal with maximums occurring at odd multiples of $1/(2\tau_d)$, and minimums occurring at even multiples of $1/(2\tau_d)$. The first minimum occurs at $f = 1/\tau_d$, and thus a measurement of this occurrence can be used to determine τ_d (21). A calibrated Gaussian noise source can be used to calibrate the system at Fourier frequencies higher than $1/(2\tau_d)$, thus extending the frequency range of this system (14,15).

The close-in noise floor of this measurement system is much larger than that of the two-oscillator system. From Eq. (47), the effective phase sensitivity of the mixer is multiplied by a factor of $2\pi f \tau_d$ and thus is less than the phase sensitivity of the two-oscillator method (21). As discussed previously, the noise floor of the two-oscillator measurement system is given by

$$S_{\phi,\mathrm{floor}}(f) = \frac{1}{k_d^2}\frac{v_n^2(f)}{\mathrm{BW}} + S_{a,A}(f)\beta_A^2 + S_{a,B}(f)\beta_B^2 \tag{53}$$

For $f \ll 1/(2\pi\tau_d)$, the noise contributions of the mixer, the amplifier, and the spectrum analyzer to the noise floor increase by a factor of $(2\pi f \tau_d)^{-2}$. The noise floor for the delay line measurement system is given by

$$S_{\phi,\mathrm{floor}}(f) = \frac{1}{(2\pi f \tau_d)^2 k_d^2}\left(\frac{v_n^2(f)}{\mathrm{BW}}\right) + S_{a,A}(f)\beta^2 \tag{54}$$

The first term usually limits the noise floor of this system. The term in large parentheses usually follows a $1/f$ power law at frequencies close to the carrier; thus the overall noise floor at these frequencies follows a f^{-3} dependence on Fourier frequency. In addition, the noise floor is inversely proportional to τ_d^2; therefore longer delays will result in lower noise floors, but also a smaller Fourier frequency span in which Eqs. (51) and (52) are valid. At very long delays, the attenuation of the signal is so large that the noise floor is adversely affected. The noise floor of this measurement system cannot be measured directly since a source is needed and the noise from the source cannot be easily separated from the noise of the measurement system. If the noise contribution of the measurement system (mixer, amplifier, and spectrum analyzer) are known, then the noise floor can be approximated using Eq. (54).

Cavity Discriminator Measurements of PM Noise in Signal Sources. Figure 15 shows a cavity discriminator measurement system (11). This system is similar to the delay-line system, but uses a high-Q cavity in place of the delay line. If the signal frequency and the cavity resonance frequency are close, the cavity causes a phase delay proportional to the signal frequency. In the linear region around ν_0, the fractional frequency fluctuations of the source are converted to phase fluctuations according to

$$\phi(t) \cong 2Qy(t) \tag{55}$$

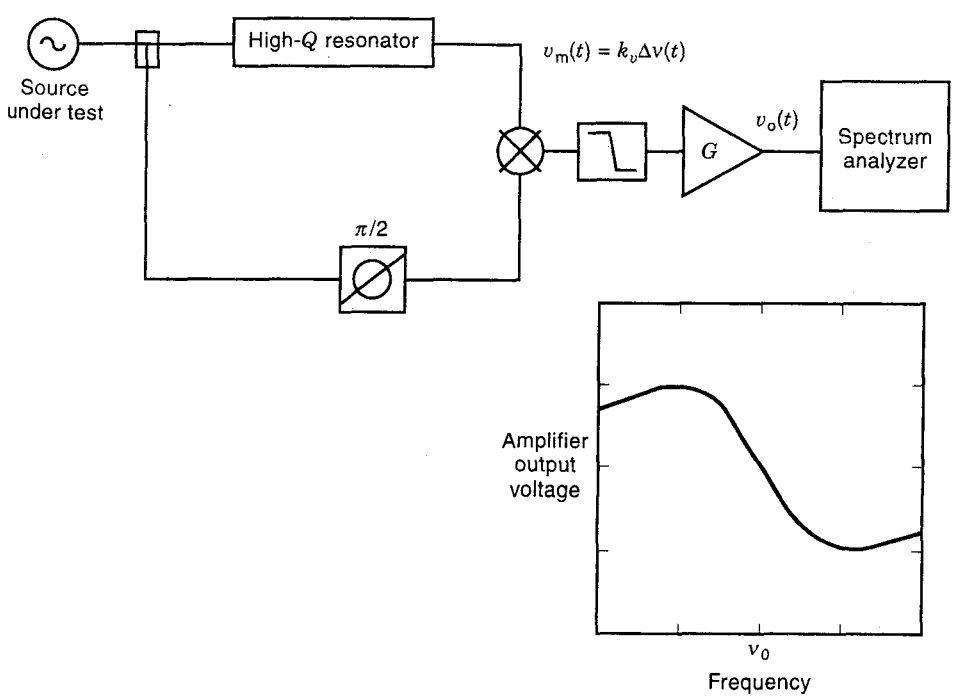

Figure 15. Block diagram of a PM noise measurement system that uses a high-Q-factor cavity to measure PM noise in an oscillator.

If the phase shifter is adjusted so that the two input signals to the mixer are in quadrature, then the output voltage of the mixer is proportional to phase fluctuations of the source. After amplification, the output voltage is given by

$$v_o(t) \cong k_d(2Q)Gy(t) = \nu_0 k_\nu G y(t) \tag{56}$$

where the mixer sensitivity to frequency fluctuations k_ν is equal to $2Qk_d/\nu_0$. (Figure 15 shows the output voltage of the amplifier as a function of input frequency.) The FM and PM noise of the source are therefore

$$S_y(f) \cong \frac{\mathrm{PSD}[v_o(t)]}{(2Qk_dG)^2} = \frac{\mathrm{PSD}[v_0(t)]}{(\nu_0 k_\nu G)^2} \tag{57}$$

$$S_\phi(f) \cong \left(\frac{\nu_0}{f}\right)^2 \frac{\mathrm{PSD}[v_o(t)]}{(2Qk_dG)^2} = \left(\frac{1}{f}\right)^2 \frac{\mathrm{PSD}[v_o(t)]}{(k_\nu G)^2} \tag{58}$$

Equations (57) and (58) are valid only for $f \ll \nu_0/(2Q)$, where the phase-to-frequency relation of the cavity is linear and k_ν is a constant. The value of k_ν can be found by stepping the frequency of the source up and down and measuring the corresponding voltage change at the output of the amplifier. The voltage change divided by the frequency change is equal to $k_\nu G$ in volts per hertz. At higher Fourier frequencies k_ν changes according to (11)

$$k_\nu \propto \frac{1}{1+\left(\dfrac{2Qf}{\nu_0}\right)^2} \tag{59}$$

A calibrated Gaussian noise source can be added to the source to calibrate the system at Fourier frequencies higher than $\nu_0/(2Q)$, thus extending the range of this measurement system.

As in the delay-line measurement system, the effective phase sensitivity of the mixer is less than the phase sensitivity of the two-oscillator method. The noise floor is thus given by

$$S_{\phi,\mathrm{floor}}(f) = \frac{1}{(2Qf)^2 k_d^2}\frac{v_n^2(f)}{\mathrm{BW}} + S_{a,A}(f)\beta^2 \tag{60}$$

Close to the carrier the noise floor follows a f^{-3} dependence on Fourier frequency and is higher than the noise of the two-oscillator measurement system. In addition, the noise floor is inversely proportional to Q^2. Therefore, higher Q cavities will result in lower noise floors, but also a smaller Fourier frequency span in which Eqs. (57) and (58) are valid. Other resonant circuits, such as multiple-pole filters, can be used in place of the cavity. The resonant circuit used can add noise to the system and thus limit the resolution or noise floor of the measurement system.

AM Noise Measurement Systems For Oscillators and Amplifiers

Simple AM Noise Measurements For Oscillators. Figure 16 shows a single-channel AM noise measurement system for a source. In this system a source drives an AM detector. The output voltage of the detector is then amplified and fed into a swept or FFT spectrum analyzer. AM detectors commonly used are the mixer detector discussed previously or a diode detector.

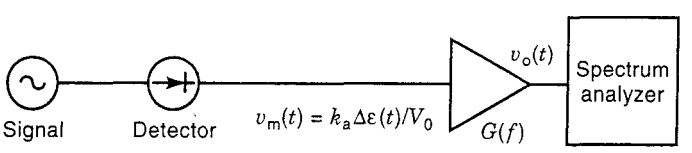

Figure 16. Block diagram of a single-channel AM noise measurement system for measuring AM noise in an oscillator.

The voltage at the output of the mixer is given by

$$v_m(t) \cong k_a \frac{\epsilon(t)}{V_0} \tag{61}$$

where k_a is the detector's sensitivity to fractional amplitude fluctuations. The AM noise of the source is then

$$S_a(f) = \frac{\mathrm{PSD}[v_o(t)]}{(k_aG)^2} \tag{62}$$

where $v_o(t)$ is the voltage into the spectrum analyzer and G is the gain of the amplifier. The sensitivity k_a can be measured by replacing the test source with a source with amplitude modulation capability (12,20). The power of the (calibration) source should be the same as the power of the test source, and it should be adjusted so that the dc voltage at the output of the mixer is the same as when the test source is used. The amplitude modulated input signal is given by

$$v(t) = V_0(1 + \mathrm{AM}_{\mathrm{in}}\cos\Omega t)\cos(2\pi\nu_0 t) \tag{63}$$

where $\mathrm{AM}_{\mathrm{in}}$ is the peak fractional amplitude modulation and Ω is the modulation frequency. The magnitude of the amplitude modulation $S_a(f)$ at the input signal is $\frac{1}{2}(\mathrm{AM})^2$, where AM is the modulation selected. The amplitude modulation at the output ($\mathrm{AM}_{\mathrm{out}}$) is then measured with the spectrum analyzer and the calibration factor is given by

$$(k_aG)^2 = \frac{2\mathrm{AM}_{\mathrm{out}}}{\mathrm{AM}_{\mathrm{in}}} \tag{64}$$

This measurement assumes that the calibration factor is a constant independent of the Fourier frequency. Many times k_a and G vary with frequency, and thus errors are introduced in the calibration. This is especially important for f higher than 100 kHz. To avoid this problem and speed the measurement of k_aG, a Gaussian noise source added to the test source can be used to calibrate the system (12,14,15). To calibrate the system, the PSD of $v_o(t)$ with the Gaussian noise on is measured with the spectrum analyzer. This curve will show any variation of k_aG with Fourier frequency if it exists. The values of $(k_aG)^2$ as a function of Fourier frequency are obtained by dividing the measured $v_o(f)$ by the known calibrated noise power.

The confidence intervals for spectrum analyzer (swept and FFT) measurements, as a function of the number of measurements, can be estimated from Table 1 (4,16–18). Biases in commonly used FFT window functions are discussed in Ref. 4.

One problem of this simple measurement system is that the measured noise, given by Eq. (62), includes the AM noise of the source in addition to noise added by the detector, the amplifier, and the analyzer (noise floor of the system). The noise components included in $S_a(f)$ are

$$S_a(f) = S_{a,\mathrm{src}}(f) + \frac{1}{(k_a)^2}\frac{v_n^2(f)}{\mathrm{BW}} \tag{65}$$

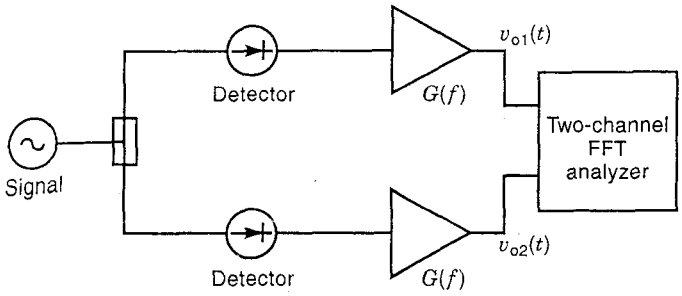

Figure 17. Block diagram of a two-channel cross-correlation system for measuring AM noise in an oscillator.

where $S_{a,src}(f)$ is the AM noise of the source, and the second term represents the noise floor of the system. It is therefore difficult to separate the AM noise of the source from the noise floor.

Cross-Correlation AM Noise Measurements For Oscillators. The noise floor of the AM noise measurement system discussed previously can be considerably reduced by using two-channel cross-correlation techniques as shown in Fig. 17. In this system PSD$[v_{o1}(t)]$ includes AM noise of the source plus noise in channel 1 (detector 1, amplifier 1). PSD$[v_{o2}(t)]$ includes AM noise of the source plus noise in channel 2 (detector 2, amplifier 2). The PSD of the cross spectrum divided by the calibration factor mainly includes the AM noise of the source since the noise that is not common between the two channels is reduced proportionally to $1/\sqrt{N}$, so

$$\frac{\mathrm{PSD}[v_{o1}(t)v_{o2}(t)]}{(k_aG)^2} = S_{a,src}(f) + \frac{1}{\sqrt{N}}\left(\frac{v_{n1}^2(t)}{(k_{a1})^2\mathrm{BW}} + \frac{v_{n2}^2(t)}{(k_{a2})^2\mathrm{BW}}\right) \quad (66)$$

This measurement technique is very useful for separating the AM noise of the source from the system noise. This system can be calibrated with a source with AM capability or by using a calibrated Gaussian noise source (12,14).

Simple AM Noise Measurements For Amplifiers. Figure 18 shows a single-channel AM noise measurement system for an amplifier. A source is used to drive the amplifier under test, and the output signal of the amplifier is fed into an AM detector. The signal is amplified, and the output voltage is measured with an spectrum analyzer. The PSD of the noise voltage $v_o(t)$ divided by the calibration factor $(k_aG)^2$ is

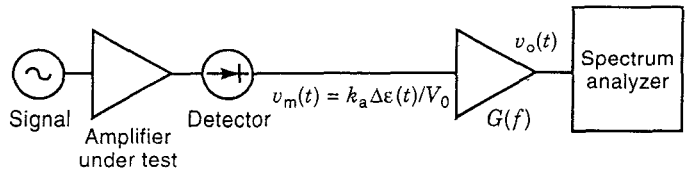

Figure 18. Block diagram of a single-channel system for measuring AM noise in an amplifier.

$$\frac{\mathrm{PSD}[v_o(t)]}{(k_aG)^2} = S_{a,src}(f) + S_{a,amp}(f) + \frac{1}{(k_a)^2}\frac{v_n^2(t)}{\mathrm{BW}} \quad (67)$$

The first term in Eq. (67) represents the AM noise of the source, the second term is the noise of the test amplifier, and the third term is the noise floor of the measurement system. The calibration factor k_aG can be obtained by using a source with AM capability or by using a calibrated Gaussian noise source to calibrate the system (12,14,20). If the AM noise of the source or the system noise floor is comparable to the amplifier noise, accurate measurements of the amplifier AM noise cannot be made using this system.

Cross-Correlation AM Noise Measurements For Amplifiers. Figure 19 shows a cross-correlation AM noise measurement system for an amplifier that reduces the noise floor of the measurement system. A reference source drives the test amplifier, the amplifier output is split, and each channel is fed into an AM detector. The output signals of the detectors are then amplified and measured with a two-channel FFT spectrum analyzer. The PSD of the cross-correlation $[v_{o1}(t)xv_{o2}(t)]$ divided by the calibration factor is

$$\frac{\mathrm{PSD}[v_{o1}(t)v_{o2}(t)]}{(k_aG)^2} = S_{a,src}(f) + S_{a,amp}(f) + \frac{1}{\sqrt{N}}\left(\frac{v_{n1}^2(t)}{(k_a)^2\mathrm{BW}} + \frac{v_{n2}^2(t)}{(k_a)^2\mathrm{BW}}\right) \quad (68)$$

Equation (68) indicates that part of the noise floor in the system is reduced by a factor of $\sqrt{N}$. If the AM noise of the source dominates the measured noise, a limiter can be placed after the source to reduce its AM noise (6).

CARRIER SUPPRESSION MEASUREMENT SYSTEMS

The concept of carrier suppression was first introduced by Sann for measuring noise in amplifiers (23). Carrier suppres-

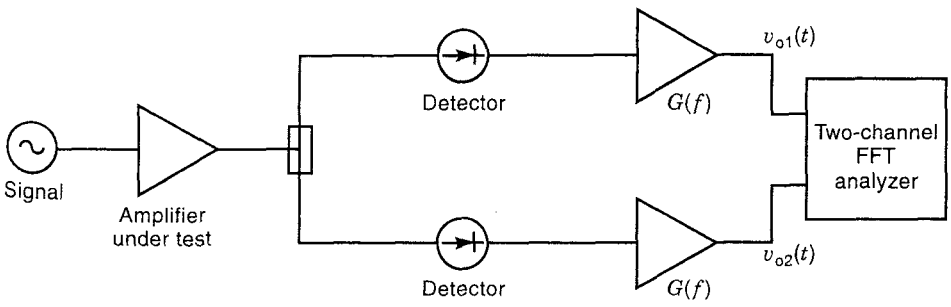

Figure 19. Block diagram of a two-channel cross-correlation system for measuring AM noise in an amplifier.

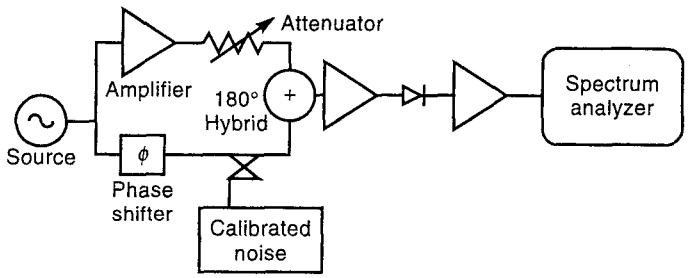

Figure 20. Carrier suppression AM noise measurement system for amplifiers.

sion measurement systems use a bridge network to cancel the power at the carrier frequency, effectively enhancing the noise of the device under test (23–26). This results in a reduction of the noise floor of the measurement system, or in other words, in an increase of the detector sensitivity.

Carrier Suppression AM Noise Measurement Systems for Amplifiers

Figure 20 shows an AM noise measurement system for amplifiers that uses carrier suppression (25). The source signal is split, and the amplifier under test is placed in one of the channels. The variable attenuator is used to match the magnitudes of the two channels. The phase shifter is used to adjust the phase difference between the two channels to 0. When the two signals are combined in the hybrid, the carrier power is mostly cancelled. The degree of cancellation depends on how well the two channels are matched. An additional amplifier is placed at the output of the power summer to increase the power input to the AM detector. The effective AM noise of the device (as seen by the AM detector) is increased by the amount of carrier suppression. An AM noise standard is used to calibrate the gain of the system.

Carrier Suppression PM Noise Measurement System for Amplifiers

Figure 21 shows a carrier suppression PM noise measurement system for amplifiers (25,26). A bridge circuit is used to effectively increase the PM noise of the amplifier with respect to the noise floor of the system. A PM noise standard is used to calibrate the gain of the system.

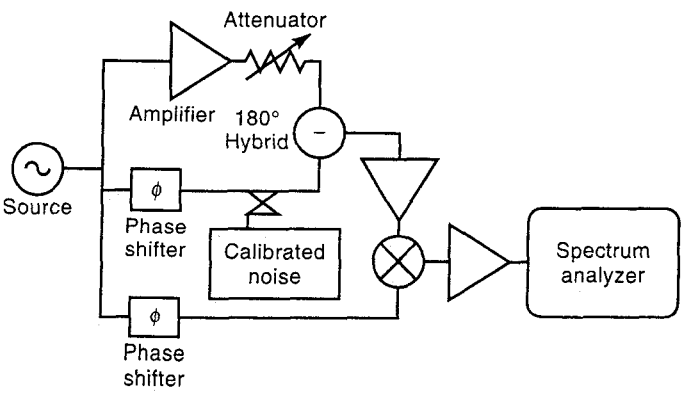

Figure 21. Carrier suppression PM noise measurement system for amplifiers.

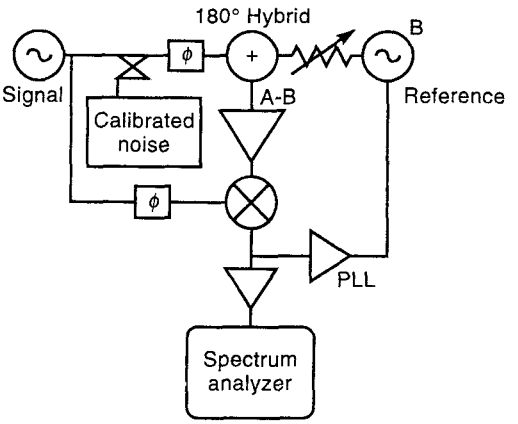

Figure 22. Two-oscillator PM noise measurement system with carrier suppression.

Carrier Suppression PM Noise Measurement Systems for Oscillators

Carrier suppression can also be used in PM measurement systems for oscillators. Figure 22 shows a two-oscillator PM noise measurement system with carrier suppression (25). In this system a bridge is used to raise the magnitude of the PM noise of the two oscillators with respect to the noise in the phase noise detector. A PM noise standard is used to calibrate the gain of the system. Carrier suppression can also be applied to delay line measurement systems (27).

The advantage of carrier suppression measurement systems over cross-correlation systems is that similar noise floors can be achieved at smaller measurement times. The disadvantage is that a very good amplitude and phase match of the bridge channels is required to suppress the carrier power. Furthermore, the match changes with temperature, and thus careful calibrations should be performed before and after a measurement to ensure that the amount of suppression has not changed. The use of a PM/AM noise standard will ease the calibration process. In some specific systems, like AM measurement systems for amplifiers, carrier suppression systems are superior. The reason is that in these systems, the AM noise of an amplifier with lower or comparable noise to the source can be accurately measured. In cross-correlation measurement systems for amplifiers it is difficult to cancel the AM noise of the source, which is often comparable or larger than the noise in the amplifier under test.

BIBLIOGRAPHY

1. E. S. Ferre-Pikal et al., Draft revision of IEEE Std 1139-1988 standard definitions of physical quantities for fundamental frequency and time metrology—random instabilities, *Proc. 1997 IEEE Frequency Control Symp.* 1997, pp. 338–357.
2. D. W. Allan et al., Standard terminology for fundamental frequency and time metrology, *Proc. 42nd Ann. Symp. Frequency Control,* 1988, pp. 419–425.
3. J. A. Barnes et al., Characterization of frequency stability, *IEEE Trans. Instrum. Meas.,* **IM-20**: 105–120, 1971.
4. D. B. Sullivan et al., Characterization of clocks and oscillators, *National Institute of Standards and Technology, Technical Note No. 1337,* 1990.

5. D. A. Howe, D. W. Allan, and J. A. Barnes, Properties of signal sources and measurement methods, *Proc. 35th Annu. Symp. Frequency Control,* 1981, pp. A1–A47; also in Ref. 4.
6. T. E. Parker, Characteristics and sources of phase noise in stable oscillators, *Proc. 41st Annu. Symp. Frequency Control,* 1987, pp. 99–110.
7. F. L. Walls and A. DeMarchi, RF spectrum of a signal after frequency multiplication; measurement and comparison with a simple calculation, *IEEE Trans. Instrum. Meas.,* **IM-24**: 210–217, 1975.
8. F. L. Walls et al., Time-domain frequency stability calculated from the frequency domain: An update, *Proc. 4th Eur. Frequency Time Forum,* 1990, pp. 197–204.
9. J. A. Barnes and D. W. Allan, Variances based on data with dead time between the measurements, *NIST Tech. Note No. 1318,* 1990; also in Ref. 4.
10. L. M. Nelson and F. L. Walls, Environmental effects in mixers and frequency distribution systems, *Proc. IEEE Frequency Control Symp.,* 1993, pp. 831–837.
11. F. L. Walls et al., Extending the range and accuracy of phase noise measurements, *Proc. 42nd Ann. Symp. Frequency Control,* 1988, pp. 432–441; also in Ref. 4.
12. L. M. Nelson, C. W. Nelson, and F. L. Walls, Relationship of AM noise to PM noise in selected RF oscillators, *IEEE Trans. Ultrason. Ferroelectr. Freq. Control,* **41**: 680–684, 1994.
13. F. L. Walls and S. R. Stein, Servo techniques in oscillators and measurement systems, *National Bureau of Standards (US) Technical Note No. 692,* pp. 1–20, 1976.
14. F. L. Walls, Secondary standard for PM and AM noise at 5, 10 and 100 MHz, *IEEE Trans. Instrum. Meas.,* **IM-42**: 136–143, 1993.
15. F. L. Walls, Reducing errors, complexity, and measurement time for PM noise measurements, *Proc. 1993 Frequency Control Symp.,* 1993, pp. 81–86.
16. D. B. Percival and A. T. Walden, *Spectral Analysis for Physical Applications,* Cambridge, UK: Cambridge University Press, 1993.
17. B. N. Taylor and C. E. Kuyatt, *National Institute of Standards and Technology,* Technical Note No. 1297, 1993.
18. F. L. Walls, D. B. Percival, and W. R. Irelan, Biases and variances of several FFT spectral estimators as a function of noise type and number of samples, *Proc. 43rd Annu. Symp. Frequency Control,* 1989, pp. 336–341; also in Ref. 4.
19. W. F. Walls, Cross-correlation phase noise measurements, *Proc. 1992 IEEE Frequency Control Symp.,* 1992, pp. 257–261.
20. F. L. Walls et al., Precision phase noise metrology, *Proc. National Conf. Standards Laboratories (NCSL),* 1991, pp. 257–275.
21. A. L. Lance, W. D. Seal, and F. Labaar, Phase noise and AM noise measurements in the frequency domain, *Infrared Millimeter Waves,* **11**: 239–289, 1984; also in Ref. 4.
22. Stanley J. Goldman, *Phase Noise Analysis in Radar Systems Using Personal Computers,* New York: Wiley, 1989, chap. 2, pp. 31–40.
23. K. H. Sann, Measurement of near-carrier noise in microwave amplifiers, *IEEE Trans. Microwave Theory and Techniques,* Vol. MTT-16, pp. 761–766, 1968.
24. G. J. Dick and J. Saunders, Method and apparatus for reducing microwave oscillator output noise, US Patent #5,036,299, July 1991. See also D. G. Santiago and G. J. Dick, Microwave frequency discriminator with a cooled sapphire resonator for ultra-low phase noise, *Proc. 1992 IEEE Freq. Control Symp.,* pp. 176–182, 1992.
25. F. L. Walls, Suppressed carrier based PM and AM noise measurement techniques, *Proc. 1997 Intl. Freq. Control Symp.,* pp. 485–492, 1997.
26. C. McNeilage et al., Advanced phase detection technique for the real time measurement and reduction of noise in components and oscillators, *Proc. 1997 IEEE Intl. Freq. Control Symp.,* pp. 509–514, 1997.
27. F. Labaar, New discriminator boosts phase noise testing, *Microwaves,* Hayden Publishing Co., Inc., Rochelle Park, NJ, **21** (3): 65–69, 1982.

FRED L. WALLS
EVA S. FERRE-PIKAL
National Institute of Standards and Technology

MEASUREMENT OF POWER. See POWER METERS.

MEASUREMENT OF WAVELENGTH. See WAVELENGTH METER.

MEASUREMENT, POWER SYSTEM. See POWER SYSTEM MEASUREMENT.

MEASUREMENTS. See CAPACITANCE MEASUREMENT; INSTRUMENTS.

MEASUREMENTS, DIELECTRICS. See DIELECTRIC MEASUREMENT.

MEASUREMENTS FOR SEMICONDUCTOR MANUFACTURING. See SEMICONDUCTOR MANUFACTURING TEST STRUCTURES.

MEASUREMENTS, GRAVITY. See GRAVIMETERS.

MEASUREMENT, SOFTWARE. See SOFTWARE METRICS.

MEASURES OF RELIABILITY. See RELIABILITY INDICES.

MECHANICAL BALANCES. See BALANCES.

MECHANIZED INFERENCE. See THEOREM PROVING.

MECHATRONICS

Mechatronics is a process for developing and manufacturing electronically controlled mechanical devices. Many of today's automated equipment and appliances are complex and smart mechatronics systems, composed of integrated mechanical and electronic components that are controlled by computers or embedded microcomputer chips. As a matter of fact, mechatronic systems are extensively employed in military applications and remote exploratory expeditions (1,2). Industrial mechatronic systems are used extensively in factory automation and robotic applications, while commercial mechatronics products are widely found in office and home appliances as well as in modern transportation. Successful systems and products are the ones that are well designed, well built, and affordable.

The term *mechatronics* was coined in 1969 to signify the integration of two engineering disciplines—*mecha*nics and ele*ctronics*. In the early 1970s, Japan was the largest ship and tanker builder in the world and its economy depended heavily on oil-driven heavy machinery and steel industries. The 1973 oil crisis saw the crude oil prices skyrocket from $3.50 per barrel to over $30.00 per barrel. The consequent disastrous impact on its oil-dependent shipping industry prompted Japan to rethink about its national economic survival and strategies. Microelectronics and mechatronics were two emerging technologies embraced by Japan as major industrial priorities after the crisis.